研究成果の刊行に関する一覧表

所属施設　国立精神・神経センター

氏　名　高坂 新一

書 籍

著者氏名	論文タイトル名	書籍全体の編集者名	書籍名	出版社名	出版地	出版年	ページ
Nakajima, K. and Kohsaka, S.	Response of microglia to brain injury.	Helmut, K., Bruce R.R.	Neuroglia	Oxford University Press	New York USA	2004	443-453
Nakajima, K. and Kohsaka, S.	Microglia: Neuroprotective and neurotrophic cells in the central nervous system.	Teruo Inoue	Current Drug Targets – Cardiovascular & Haematological Disorders	Bentham Science Publishers Ltd.		2004	65-84

雑 誌

発表者氏名	論文タイトル名	発表誌名	巻号	ページ	出版年
Hirasawa, T., Ohsawa, K., Imai, Y., Ondo, Y., Uchino, S. and Kohsaka, S.:	Visualization of microglia in living tissues by using Iba-1EGFP transgenic mice.	J. Neurosci. Res.		in press	2005
Kamitori, K., Tanaka, M. and Kohsaka, S.:	Receptor related to tyrosine kinase RYK regulates cell migration during cortical development	BBRC	330	439-445	2005
Azuma, N., Tadokoro, K., Asaka, A., Yamada, M., Yamaguchi., Handa, H., et al.	The Pax6 isoform bearing an alternative spliced exon promotes the development of the neural retinal structure.	Hum. Mol. Genet.	14	735-745	2005
Nakajima, K., Tohyama, Y., Kurihara, T. and Kohsaka, S.:	Axotomy-dependent urokinase induction in the rat facial nucleus: possible stimulation of microglia by neurons.	Neurochem Int.	46	107-116	2005
Akazawa, C., Tsuzuki, H., Nakamura, Y., Sasaki Y., et al.	The upregulated expression of sonic hedgehog in motor neurons after rat facial nerve axotomy.	J. Neurosci.	24	7923-7930	2004
Akazawa, C., Nakamura, Y., Sango, K., Horie, H. and Kohsaka, S.:	Distribution of the galectin-1 mRNA in the rat nervous system; its transient upregulation in rat facial motor neurons after facial nerve axotomy..,	Neurosci	125	171-178	2004

研究成果の刊行に関する一覧表

所属施設 国立精神・神経センター

氏　名 和田 圭司

雑 誌

発表者氏名	論　文　タ　イ　ト　ル　名	発 表 誌 名	巻　号	ペ　ー　ジ	出版年
Harada, T., Harada, C., et al.	Role of ubiquitin carboxy terminal hydrolase-L1 in neural cell apoptosis induced by ischemic retinal injury *in vivo*.	Am. J. Pathol	164	59-64	2004
Kwon, J., Wang, Y.L, et al.	Two closely related ubiquitin C-terminal hydrolase isozymes function as reciprocal modulators of germ cell apoptosis in cryptorchid testes..	Am. J. Pathol.	164	1367-1374	2004
Manago, Y., Kanahori, Y. et al.	Potentiation of ATP-induced currents due to the activation of P2Xreceptors by ubiquitin carboxy-terminal hydrolase L1.	Journal of Neurochemistry	in press		2005

研究成果の刊行に関する一覧表

所属施設 岐阜薬科大学分子生物学
氏　名 古川 昭栄

雑 誌

発表者氏名	論文タイトル名	発表誌名	巻号	ページ	出版年
Yamada, Y., Shimizu, K., Nitta, A., Soumiya, H., Fukumitsu, H., Furukawa, S.	Axonal regrowth downregulates the synthesis of glial cell line-derived neurotrophic factor in the lesioned rat sciatic nerve.	Neurosci. Lett.	364	11-15	2004
Kinukawa, H., Jikou, T., Nitta, A., Furukawa, Y., Hashimoto, M., Fukumitsu, H., Nomoto, H., Furukawa, S.	cAMP/protein Kinase A signal attentuates Ca^{2+}-induced fibroblast growth factor-1 synthesis in rat cortical neurons.	J. Neurosci. Res.	77	487-497	2004
Nitta, A., Nishioka, H., Fukumitsu, H., Furukawa, Y., Sugiura, H., Shen, L., Furukawa, S.	Hydrophobic dipeptide, Leu-Ile, protects against neuronal death by inducing BDNF and GDNF synthesis.	J. Neurosci. Res.	78	250-258	2004

研究成果の刊行に関する一覧表

所属施設　慶應義塾大学

氏　名　島崎 琢也

雑 誌

発表者氏名	論文タイトル名	発表誌名	巻号	ページ	出版年
Uemura, O., Okada, Y., Ando, H., Guedj, M., Higashijima, S., Shimazaki, T., Chino, N., Okano, H., Okamoto, H.	Comparative functional genomics revealed conservation and diversification of three enhancers of the isl1 gene for motor and sensory neuron-specific expression.	Dev. Biol.	278	587-606	2005
Okada, Y., Shimazaki, T., Sobue, G., Okano, H.	Retinoic-acid-concentration-dependent acquisition of neural cell identity during in vitro differentiation of mouse embryonic stem cells.	Dev. Biol.	275	124-142	2004
Ishibashi, S., Sakaguchi, M., Kuroiwa, T., Yamasaki, M., Kanemura, Y., Shizuko, I., Shimazaki, T., Onodera, M., Okano, H., Mizusawa, H.	Human neural stem/progenitor cells, expanded in long-term neurosphere culture, promote functional recovery after focal ischemia in Mongolian gerbils.	J. Neurosci. Res.	78	215-223	2004
Yoshizaki, T., Inaji, M., Kouike, H., Shimazaki, T., Sawamoto, K., Ando, K., Date, I., Kobayashi, K., Suhara, T., Uchiyama, Y., Okano, H.	Isolation and transplantation of dopaminergic neurons generated from mouse embryonic stem cells.	Neurosci. Lett.	363	33-37	2004

研究成果の刊行に関する一覧表

所属施設　東京大学
氏　名　久恒 辰博

雑誌

発表者氏名	論文タイトル名	発表誌名	巻号	ページ	出版年
Imura, T., Kanatani, S., Fukuda, S., Miyamoto, Y., Hisatsune, T.	Layer-specific production of nitric oxide during cortical circuit formation in postnatal mouse brain	Cerebral Cortex	15	332-340	2005
Yoshida, M., Fukuda. S., Tozuka, Y., Miyamoto, Y., Hisatsune, T.	Developmental shift in bidirectional functions of taurine-sensitive chloride channels during cortical circuit formation in postnatal mouse brain	J. Neurobiol.	60	166-175	2004

研究成果の刊行に関する一覧表

所属施設　京都大学医学研究科
氏　名　高橋 淳

雑 誌

発表者氏名	論文タイトル名	発表誌名	巻号	ページ	出版年
Kishi, Y., Takahashi, J., Koyanagi, M., Morizane, A., Okamoto, Y., Horiguchi, S., Tashiro, K., Honjo, T., Fujii, S., Hashimoto, N.	Estrogen promotes the differentiation and survival of dopaminergic neurons derived from human neural stem cells.	J. Neurosci. Res.	79(3)	279-286	2005
Takagi, Y., Takahashi, J., Saiki, H., Morizane, A., Hayashi, T., Kishi, Y., Fukuda, H., Okamoto, Y., Koyanagi, M., Ideguchi, M., Hayashi, H., Imazato, T., Kawasaki, H., Suemori, H., Omachi, S., Iida, H., Itoh, N., Nakatsuji, N., Sasai, Y., Hashimoto, N.	Dopaminergic neurons generated from monkey embryonic stem cells function in a Parkinson primate model.	J. Clin.. Invest.	115(1)	102-109	2005

Ⅳ. 研究成果の刊行物・別刷

Neuroscience 125 (2004) 171–178

DISTRIBUTION OF THE GALECTIN-1 mRNA IN THE RAT NERVOUS SYSTEM: ITS TRANSIENT UPREGULATION IN RAT FACIAL MOTOR NEURONS AFTER FACIAL NERVE AXOTOMY

C. AKAZAWA,[a]* Y. NAKAMURA,[a] K. SANGO,[b] H. HORIE[c] AND S. KOHSAKA[a]

[a]*Department of Neurochemistry, National Institute of Neuroscience, NCNP, Japan, Ogawahigashi 4-1-1, Kodaira, Tokyo 187-8502, Japan*

[b]*Department of Developmental Morphology, Tokyo Metropolitan Institute for Neuroscience, Musashidai 2-6, Fuchu, Tokyo 183-8526, Japan*

[c]*Institute for Biomedical Science, Waseda University, Higashifushimi 2-7-5, Nishi-Tokyo, Tokyo 202-0021, Japan*

Abstract—Galectin-1 is a member of the animal lectin family that displays conserved consensus sequences and similar carbohydrate binding specificities. Recent analyses revealed that galectin-1 plays an important role in the process of nerve regeneration. We analyzed the topological expression of galectin-1 mRNA in adult rat nervous system. Galectin-1 mRNA was predominantly observed in the cell bodies of neurons such as oculomotor nucleus (III), trochlear nucleus (IV), trigeminal motor nucleus (V), abducens nucleus (VI), facial nucleus (VII), hypoglossal nucleus (XII), red nucleus, and locus ceruleus. Neurons in pineal gland and dorsal root ganglia expressed galectin-1 mRNA. We next tested whether the axotomy of facial nerve altered the expression of galectin-1 mRNA in motor neurons. In the adult rats, the axotomy of facial nerve induced transient upregulation of galectin-1 mRNA around 6 h after axotomy. These results indicate that galectin-1 may play roles in the early event of the nerve injury and regeneration through the transient change of its expression level.

Key words: galectin-1, *in situ* hybridization, facial nerve axotomy, motor neuron.

Animal lectins can be classified into two protein families on the basis of their carbohydrate recognition properties (Drickamer, 1988). The first group of calcium-dependent lectins constitutes a large class of integral membrane proteins which include the mammalian asialoglycoprotein receptors and the selectins (Lasky, 1992). The second group of lectins displays the specificity for lactose derivatives in a calcium independent manner (Barondes, 1984). The biological properties of surface carbohydrates have been shown to regulate inflammation, cell adhesion, cell proliferation, cell death, and regeneration of damaged tissues (for review, cf. Hirabayashi and Kasai, 1993; Caron et al., 1990). Galectin, a member of animal lectins, form a molecular family bearing their properties specific for galactosides. Galectins had been called by different names depending on the researchers (e.g. electrolectin, soluble lectins, galaptins, S-Lac lectins, β-galactoside-binding lectins, S-type lectins, etc.), although they have homologous sequences to each other. In order to avoid further inconvenience and confusion, the researchers agreed to use the term galectin (Barondes, 1994). Evidence suggests that the biological activities of the galectins are related to their multivalent binding capacities since most galectins possess two carbohydrate recognition domains. For example, galectin-1 which forms a homomeric dimer binds and cross-links its specific glycoprotein counter-receptors on the surface of human T-cells leading to apoptosis (Amano et al., 2003).

There are several lines of evidence relating galectin-1 to the axonal growth during the developing brain and the nerve regeneration. It was previously reported that galectin-1 localized in the CNS and peripheral nervous system (PNS) in the developmental stages, meanwhile its expression was down-regulated and restricted to PNS in the adult brain (Dodd and Jessell,1986; Hynes et al., 1990). In the olfactory system, galectin-1 has been shown to promote neurite outgrowth in the developing mouse (Puche and Key, 1995). More direct evidence for galectin-1 being involved in axonal growth came from the recent study by using recombinant human galectin-1 to promote axonal regeneration after nerve injury both *in vitro* and *in vivo* (Horie et al., 1999). The non-reducing condition of galectin-1 shows its high potency to promote the axonal regeneration of adult dorsal root ganglia explants at low concentrations (50 pg/ml) that are two orders of magnitude lower than those of the lectin activity of reduced galectin-1, suggesting that galectin-1 may act as a cytokine and not as a lectin.

In the course of analyzing galectin-1 expression, we found that the galectin-1 mRNA was expressed in the discrete population of neurons in adult CNS. Its expression was transiently upregulated in the facial motor neurons after the facial nerve axotomy, suggesting its role after the nerve injury.

*Corresponding author. Tel: +81-423-41-2711; fax: +81-425-67-0518.
E-mail address: akazawa@ncnp.go.jp (C. Akazawa).

Abbreviations: ac, anterior commissure; CA1–3, fields CA1–3 of Ammon's horn; Cb, cerebellar cortex; cc, corpus callosum; CN, deep cerebellar nuclei; Cx, cerebral cortex; DG, dentate gyrus; DR, dorsal raphe nucleus; 4th, 4th ventriculus; Hi, hippocampus; IC, inferior colliculus; MoV, motor trigeminal nucleus; NG, nodose ganglia; OB, main olfactory bulb; Or, stratum oriens; PNS, peripheral nervous system; Po, posterior thalamic nucleus; PR, pontine reticular nucleus; Py, stratum pyramidale; R, red nucleus; Ra, stratum radiatum; SC, superior colliculus; SN, substantia nigra; SSC, sodium chloride/sodium citrate; St, striatum; TG, trigeminal ganglia; Th, thalamus; TM, tuberomammillary nucleus; V, lateral ventricle.

0306-4522/04$30.00+0.00 © 2004 IBRO. Published by Elsevier Ltd. All rights reserved.
doi:10.1016/j.neuroscience.2004.01.034

EXPERIMENTAL PROCEDURES

All procedures in this study were approved by the ethical committee upon animal experiments of the National Institute of Neuroscience, NCNP, Japan. The number of animals used was minimized to include only that number needed to ensure reproducibility of results; the suffering was minimized by use of inhaled ether.

Northern blot analysis

Northern blot analyses using ^{32}P-labeled DNA probes was carried out as described previously (Akazawa et al., 1994). The template used for the random primer labeling was the same as used for the riboprobe synthesis for *in situ* hybridization. Total RNA was isolated from pooled materials dissected from the brains of adult Wistar rat by GTC-phenol extraction method as described in detail elsewhere (Chomczynski and Sacchi, 1987), and 30 μg of the total RNA was electrophoresed in a formaldehyde/1.2% agarose gel and transferred to a nylon membrane (Hybond N$^+$; Amersham Biosciences, Piscataway, NJ, USA). The hybridization was carried out at 42 °C containing 50% formamide, 5× sodium chloride/sodium citrate (SSC). The filter was washed under the high stringency of 0.1× SSC, 1% SDS, at 65 °C for 1 h.

In situ hybridization

In situ hybridization was carried out in a way similar to that described elsewhere (Akazawa et al., 1994). Female Wistar rats (200–300 g) were deeply anesthetized with ether and decapitated. Tissues were immediately removed and flash frozen in isopentane at −70 °C. Sections of 14-μm thickness were cut on a cryostat and thaw-mounted onto siran-coated slides, following briefly air-dried and kept in −80 °C until use. Adjacent series of the sections were stained with Nissl and used to confirm the cryoarchitecture and to identify the region in comparison with the references (Paxinos and Watson, 1986).

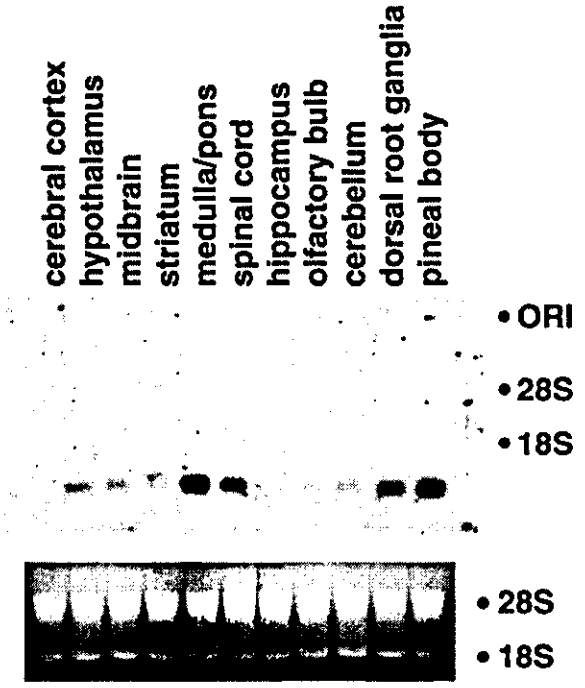

Fig. 1. Northern blot analysis of galectin-1 in rat brain (Top). Each lane contained 30 μg of total RNA purified from the pooled material respectively indicated above. As a molecular size standard, the position of origin (ORI), 28S (5.1 kbp), and 18S (2.0 kbp) were indicated. Ethidium bromide staining of the gel showed that relatively equal amount of RNA with no degradation was loaded in this experiment (bottom).

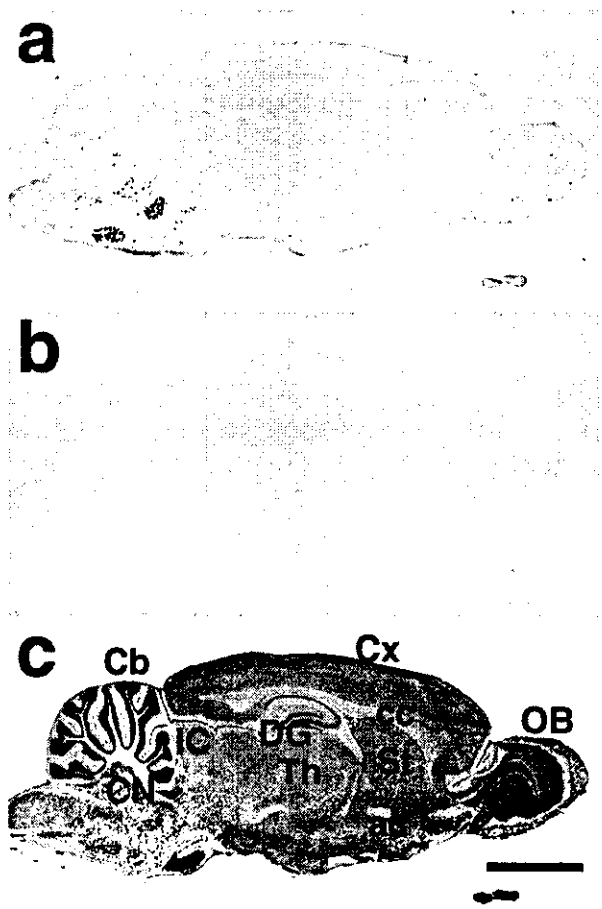

Fig. 2. Distribution of galectin-1 transcripts in the lower magnitude images of parasagittal section of adult rat brain. Sections were hybridized with an antisense riboprobe corresponding to the 408 bp of full-length galectin-1 cDNA (a) or with a sense riboprobe (b). An adjacent section was stained with Nissl (c). Cb, cerebellar cortex; CN, deep cerebellar nuclei; Hi, hippocampus; LS, lateral septal nuclei; OB, main olfactory bulb; RS, retrosplenial cortex; SN, substantia nigra; Th, thalamus. Scale bar=4 mm.

The full coding length of rat Galectin-1 cDNA (408 bp) was amplified by PCR using paired primers (5′-ATGGCCTGTGGTCTGGTCGCC-3′, and 5′-TCACTCAAAGGCCACACACTT-3′). The amplified fragment was subcloned to pGEM-T easy vector (Promega, Madison, WI USA) and subsequently sequenced. The anti-sense and sense riboprobes were synthesized by transcription using either T7 or SP6 RNA-polymerase (Roche Diagnostics GmbH, Mannheim, Germany) in the presence of digoxigenin-UTP (Roche Diagnostics GmbH) for 30 min at 37 °C, according to the manufacturer's protocol. The digoxigenin-labeled RNA probe was column-purified and reconstituted in distilled water at the concentration of 0.1 μg/ml. Sections were fixed in 4% paraformaldehyde in 0.1 M PBS for 20 min, washed in PBS, and hybridized overnight at 65 °C in a mixture (50% formamide, 10 mM PBS, 20 mM Tris–HCl, pH 7.4, 5 mM EDTA, 10% dextran sulfate, 1× Denhardt's reagents, 0.2% sodium lauryl sarcosine, 500 μg/ml t-RNA, 200 μg/ml sonicated single strand-DNA) containing digoxigenin-labeled probe (0.5 μg/μl hybridization mixture). After hybridization, sections were washed in 10 mM dithiothreitol in 5× SCC at 55 °C. After washing, alkaline phosphatase-conjugated anti-digoxigenin antibody staining was performed following the

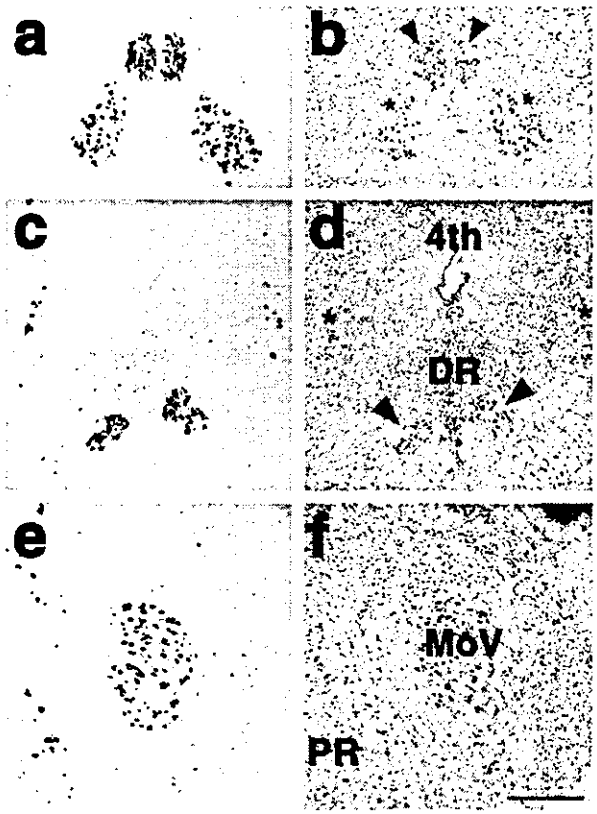

Fig. 3. Hybridization with antisense riboprobe (a, c, and e) and control Nissl staining (b, d, and f) of adult rat coronal sections. Arrowheads in b indicate oculomotor nucleus. * in b indicate red nucleus magnocellulare (a, b). Arrowheads in d indicate trochlear nucleus. * in d indicates mesencephalic trigeminal nucleus. DR, dorsal raphe nucleus; MoV, motor trigeminal nucleus; PR, pontine reticular nucleus; 4th, 4th ventriculus (c, d). Scale bar=0.2 mm.

chromogenic reaction containing Nitroblue Tetrazolium and 5-bromo-4-chloro-3-indolylphosphate. After capturing the images, sections were counter-stained with Nissl, dehydrated in a graded series of ethanol, and coverslipped with DePeX (Gurr; BDH, Poole, UK).

Facial nerve transection

Under ether anesthesia, the facial nerve was transected at the stylomastoid foramen. In all experiments, the un-operated contralateral side served as a control. After the indicated time intervals (3, 6, 9, 12, 24 h), rats were killed under the deep anesthesia by ether. The brains were quickly removed without perfusion and frozen at −70 °C until use. For the Northern blot analysis, bilateral facial nuclei were identified under the microscope, and punched out by 18 gauge needle. Three independent rats were operated and pooled facial nuclei were subjected to the total RNA preparation. Northern blot analysis using 10 μg of total RNA was carried out. The radioactive intensity was measured by BAS5000 image analyzer (Fuji, Tokyo, Japan).

RESULTS

Northern blot analysis

The full coding region of rat galectin-1 was radiolabeled by the random primer labeling method and hybridized with the membrane blotted with 30 μg of total RNA purified from the

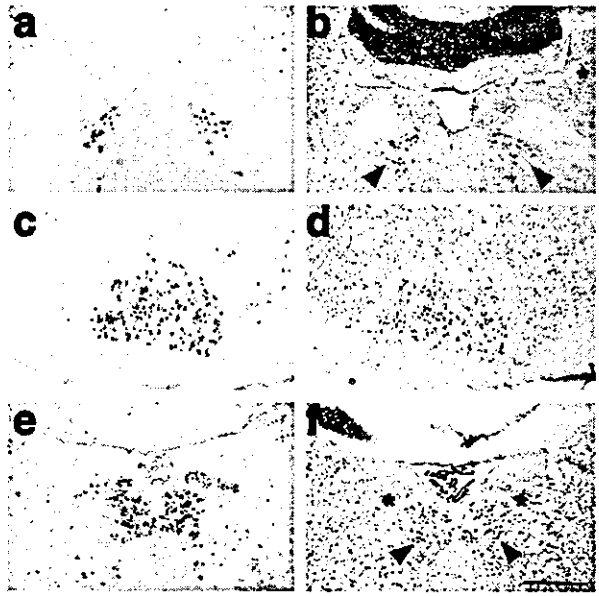

Fig. 4. Hybridization with antisense riboprobe (a, c, and e) and control Nissl staining (b, d, and f) of adult rat coronal sections. Arrowheads in b indicate abducens nucleus. * in b indicates medial vestibular nucleus. Facial nucleus was positively stained with galectin-1 (c, d). Arrowheads in f indicate hypoglossal nucleus. * in f indicates dorsal motor nucleus of vagus. The choroidal plexus was moderately stained with galectin-1 (e, f). Scale bar=0.2 mm.

various brain regions of adult rat. Galectin-1 mRNA was detected as a single band corresponding to the molecular weight of 1,000 base-pairs in the discrete brain regions, such as medulla/pons, pineal body, spinal cord and dorsal root ganglia (Fig. 1, top). Ethidium bromide staining of the gel showed that relatively equal amount of RNA was loaded (Fig. 1, bottom). The band intensity of cerebral cortex and hippocampus was significantly lower than other lanes tested.

In situ hybridization

The digoxigenin-labeled cRNA probe was hybridized with the para-sagittal section of the adult rat. The antisense riboprobes displayed the punctuated staining in the brain stem lesions (Fig. 2a), while no specific staining was detected in the section hybridized with sense ribo-probes hybridized with the adjacent section (Fig. 2b). The hybridization experiment with the same labeled antisense riboprobe in the presence of 100-fold excess of unlabeled probes resulted in no significant signals (data not shown). Neurons expressing galectin-1 mRNA were observed in strictly limited areas throughout the rat brain (summarized in Table 1). The most densely stained cells were seen in the neurons resided at the brainstem. No apparent hybridization signals were observed on glial cells from our experimental condition.

Olfactory system

In the adult rat olfactory bulb, galectin-1 mRNA was detected in mitral cells, external tufted cells, granule cells and cells in the glomerular layer (data not shown), although the

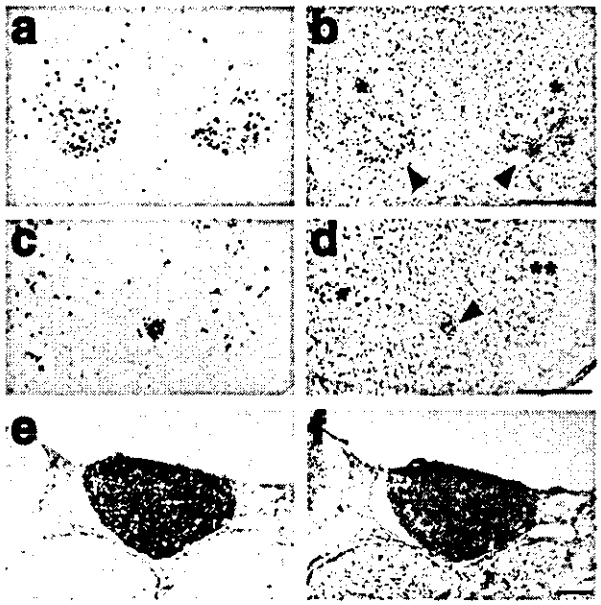

Fig. 5. Hybridization with antisense riboprobe (a, c, and e) and control Nissl staining (b, d, and f) of adult rat coronal sections. Red nucleus complex was positively stained with galectin-1. Arrowheads in b indicate magnocellulare of red nucleus and * in b indicates parvicellular of red nucleus. The arrowhead in d indicates ambiguis nucleus. * intermediate reticular nucleus. ** parvicellular reticular nucleus. Pineal body (epiphysis) was intensely stained with galectin-1 (e, f). Pea mater was moderately stained.

level of expression was not intense compared with the other brain regions. The results were identical with the previous report (Puche and Key, 1995).

Cerebral cortical areas

The expression of galectin-1 mRNA was essentially same throughout the neocortex and allocortex. The scattered staining pattern was detected in the layers IV–VI (data not shown), although the signal intensities were very weak. In the hippocampus formation, the expression of galectin-1 mRNA was barely detected (Fig. 6a).

Subcortical regions in the forebrain

Neuronal cell bodies of some regions were weakly labeled in the septum and amygdaloid complex including the endopiriform nuclei. In the preoptic and hypothalamic regions, neuronal cell bodies were weakly labeled with galectin-1 mRNA in paraventricular nucleus, arcuate nucleus and tuberomammillary nucleus. In the habenula, no labeled neuron was detected.

Lower brain stem

The signal intensities of galectin-1 positive neurons in the midbrain were stronger than those in the forebrain regions. Neuronal cell bodies of oculomotor nucleus (arrowheads in Figs. 3a and 3b) and magnocellular red nucleus (asterisks in Figs. 3a and 3b) showed prominent expression of galectin-1 mRNA. Neurons in dorsal raphe nucleus displayed weak expression of galectin-1 mRNA

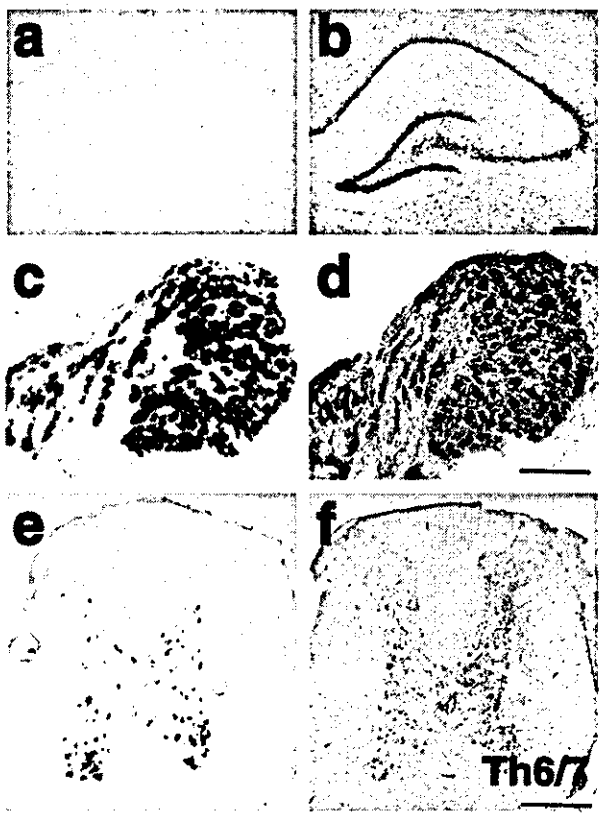

Fig. 6. Hybridization with antisense riboprobe (a, c, and e) and control Nissl staining (b, d, and f) of adult rat coronal sections. No significant staining was observed in hippocampal formation (a, b). Neurons in dorsal root ganglia were intensely stained with galectin-1 (c, d). Ventral motor neurons were positively stained in the spinal cord (thoracic: th6/7). Scale bar=0.2 mm.

while neurons in trochlear nucleus (arrowheads in Fig. 3c and 3d) and mesencephalic reticular formation (asterisks in Fig. 3c and 3d) shows intense staining. As shown in Fig. 3e and 3f, neurons in pontine reticular formation and trigeminal motor nucleus expressed galectin-1 mRNA at high level. (Fig. 4a–f).

Spinal cord, dorsal root ganglia and autonomic ganglia

In the PNS, the galectin-1 mRNA was detected in the nucleus motorius lateralis at the level of cervical to sacral spinal cord. All the neurons of dorsal root ganglia expressed galectin-1 mRNA, while possible glial cells of small size did not seem to be labeled in this experimental condition. To further access the expression of galectin-1 in peripheral sensory neurons, trigeminal ganglia (TG) and nodose ganglia (NG) were analyzed by *in situ* hybridization analysis. The neurons of TG and NG did not show any signal of galectin-1 mRNA (data not shown). We also examined the autonomic ganglion neurons such as superior cervical ganglia and sphenopalatine ganglia and galectin-1 mRNA could not be detected (data not shown).

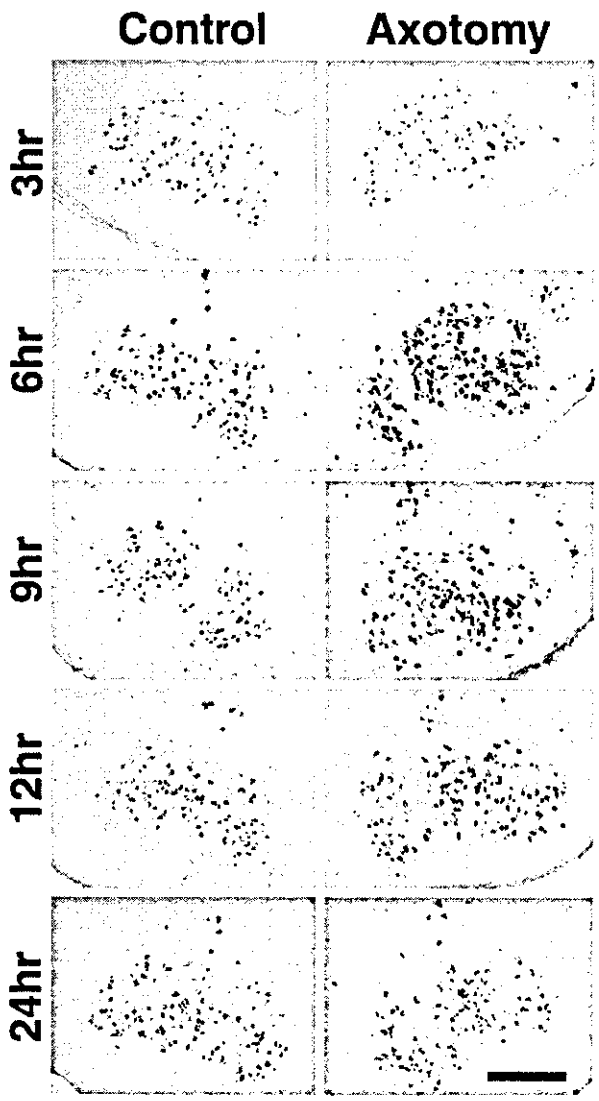

Fig. 7. Coronal sections containing bilateral facial nuclei were examined by *in situ* hybridization. The galectin-1 mRNA expression was transiently (6 h and 9 h after axotomy) upregulated in the motor neurons of the axotomized facial nucleus. No upregulation was detected in the control side. Scale bar=2 mm.

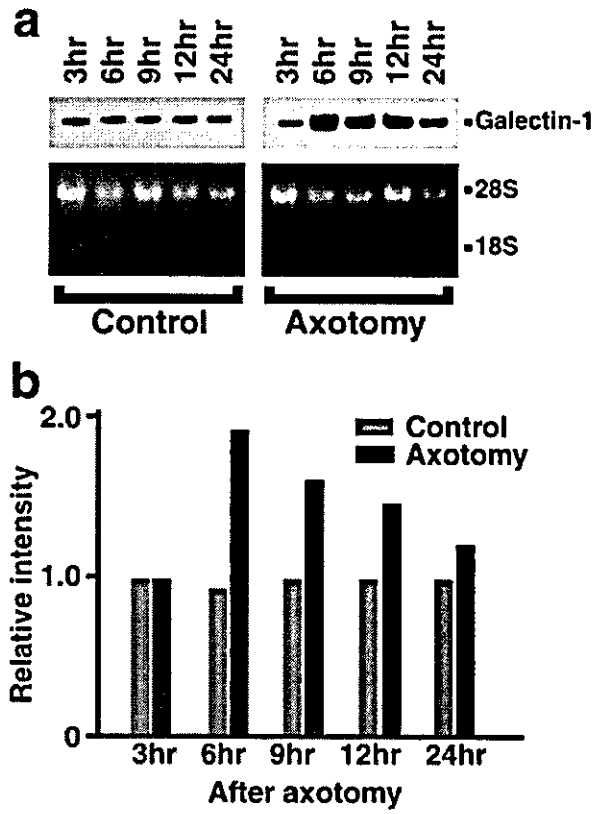

Fig. 8. Northern blot analyses were carried out to confirm the upregulation of galectin-1 mRNA (a). The bands corresponding to the 6 h to 9 h after axotomy significantly upregulated the galectin-1 mRNA compared with the non-operated control side (Top). The ethidium bromide staining of the gel indicated that the relatively equal amount of total RNA was loaded in this experiment (bottom). The radioactive intensity was measured using the image analyzer and plotted against time course after axotomy (b). Relative intensity per control (3 h) was shown. On the side of operation, the level of galectin-1 mRNA was increased by two-fold after 6–9 h after the facial nerve axotomy. Boxed: axotomy; Gray: control.

Non-neuronal cells

In addition to the neuronal expression, pinealocytes in the pineal gland expressed the high level of galectin-1 mRNA (Fig. 5e and 5f).

Axotomy of facial nerve and isciadic nerve

Following hemilateral axotomy of facial nerve at the surface of stylomastoideus foramen, the expression of galectin-1 mRNA in the facial nuclei was analyzed by the *in situ* hybridization analysis. Only on the side of the operation, facial neurons gave rise to a significant signal around 6 h and 9 h incubation after axotomy. No significant increase of galectin-1 mRNA was detected after 24 h incubation after axotomy (Fig. 7). To quantify the level of galectin mRNA, the Northern blot analysis was performed. The total RNA purified from the pooled facial nuclei from three independent experiments was analyzed at the indicated intervals after axotomy (3 h, 6 h, 9 h, 12 h, and 24 h). Expression of galectin-1 mRNA was upregulated from 6 h to 9 h interval after axotomy only on the side of the operation. By contrast, the opposite side of the facial nuclei did not show any increase of galectin-1 mRNA. The radioactive intensity was quantified using BAS5000 image analyzer and plotted against the time course after the axotomy. The level of galectin-1 mRNA was increased by two-fold compared with the non-operated control side (Fig. 8b). The ethidium bromide staining of the electrophoresed gel showed that the relatively equal amount of total RNA were loaded in this experiment (Fig. 8a, bottom).

DISCUSSION

Galectin-1 was described as a β-galactoside binding animal lectin, exhibiting its lectin activity only when it is reduced. Previously, it was reported that galectin-1 acts as a repair factor in peripheral nerve axotomy (Horie et

Table 1. Distribution of galectin-1 mRNA in the rat nervous system

Regions in the CNS examined[a]	Relative intensity on cell bodies[b]
Olfactory system	
Main olfactory bulb	
Mitral cells	1
Tufted cells	1
Granule cells	1
Scattered small cells	1
Accessory olfactory bulb	0
Anterior olfactory nucleus	0
Olfactory tubercle	
Pyramidal cells	0
Islands of Calleja	1
Neocortex	1
Limbic cortex	
Piriform cortex	1
Cingulate cortex	1
Retrosplenial cortex	1
Perirhinal cortex	0
Entorhinal cortex	0
Parasubicular cortex	0
Dentate gyrus	
Granule cells	0
CA4	0
Ammon's horn (CA1–CA3)	0
Septum	
Lateral septal nucleus	1
Medial septal nucleus	1
Septohypothalamic nucleus	0
Septofimbrial nucleus	1
Triangular septal nucleus	0
Nuclei of the diagonal band	0
Bed nucleus of the stria terminalis	1
Preoptic region	0
Amyglada	
Anterior amygdaloid area	1
Nucleus of the lateral olfactory tract	1
Cortical amygdaloid nucleus	1
Medial amygdaloid nucleus	0
Bed nucleus of the accessory olfactory tract	0
Posteromedial cortical amygdaloid nucleus	0
Lateral amygdaloid nucleus	1
Basolateral amygdaloid nucleus	
Ventral part	0
Other parts	0
Basomedial amygdaloid nucleus	1
Central amygdaloid nucleus	1
Dorsal endopiriform nucleus	1
Ventral endopiriform nucleus	1
Basal ganglia	
Caudate-putamen	0
Nucleus accumbens	1
Ventral pallidum	0
Globus pallidus	1
Entopenduncular nucleus	0
Subthalamic nucleus	0
Claustrum	0
Substantia nigra	1
Zona incerta	0
Hypothalamus	
Anterior hypothalamic area	0
Lateral hypothalamic area	0

Table 1. continued

Regions in the CNS examined[a]	Relative intensity on cell bodies[b]
Suprachiasmatic nucleus	0
Supraoptic nucleus	0
Paraventricular nucleus	1
Periventricular nucleus	0
Arcuate nucleus	1
Ventromedial hypothalamic nucleus	1
Dorsomedial hypothalamic nucleus	0
Tuberomammilllary nucleus	1
Premammillary nucleus	0
Medial mammillary nucleus	0
Lateral mammillary nucleus	0
Habenula	
Medial habenular nucleus	0
Lateral habenular nucleus	0
Thalamus	
Thalamic reticular nucleus	1
Other nuclei	0
Lower brain stem	
Pretectum	
Anterior pretectal nucleus	1
Other nuclei	0
Red nucleus	3
Acueductal gray	0
Superior colliculus	0
Inferior colliculus	0
Nucleus of brachium of inferior colliculus	0
Mesencephalic reticular formation	
Ventral tegmental area	
Interpeduncular nucleus	
Parabrachial nuclei	
Oculomotor nucleus	3
Trochlear nucleus	3
Locus cereus	1
Laterodorsal tegmental nucleus	0
Barrington's nucleus	0
Nucleus O	0
Superior olivary nuclei	1
Nucleus of trapezoid body	0
Pontine reticular formation	3
Pontine tegmental reticular nucleus	2
Pontine nucleus	1
Abducens nuclei	3
Paragenual nucleus	0
Raphe nuclei	0
Medullary reticular formation	3
Trigeminary sensory complex	0
Trigeminal motor complex	3
Cochlear nuclei	
Dorsal nucleus	3
Ventral nucleus	3
Facial nucleus	3
Vestibular nuclei	0
Prepositus hypoglossal nucleus	3
Inferior olivary nuclei	1
Ambiguus nucleus	3
Nucleus of the solitary tract	1
External cuneate nucleus	0
Cuneate nucleus	0
Gracile nucleus	0
Cerebellum	

Table 1. continued

Regions in the CNS examined[a]	Relative intensity on cell bodies[b]
Deep nuclei	3
Cortex	
Purkinje cells	0
Granular cells	0
Golgi cells	0
Stellate cells	0
Spinal cord (C–S)	
Substantia gelatinosa	0
Ventral horn	2
Motor neurons	3
Central gray	0

[a] The brain regions were demarcated according to Paxinos and Watson (1986).
[b] Relative intensity on cell bodies: 3, very high; 2, high; 1, low; 0, background level.

al., 1999). Galectin-1 enhances axonal regeneration after nerve injury through promoting the reactive Schwann cells to migrate. But the expression analyses of galectin-1 in the nervous system were only limited in restricted areas. Thus we focused our attention on the topological analysis of galectin-1 mRNA in the brain. Immunohistochemistry using galectin-1 antibody cannot address the cell types that produce galectin-1, because galectin-1 was secreted from cells. Although the molecular mechanisms of galectin-1 secretion, even without signal leading peptide, were characterized in the case of muscle cells (Cooper and Barondes, 1990), the detailed molecular mechanisms remain to be solved. Thus *in situ* hybridization analysis is the only way to identify the galectin-1 producing cells. As previously reported, galectin-1 mRNA was detected at a high level in the discrete population of neurons of cerebral nuclei. Furthermore, galectin-1 was detected in cortical neurons at low level not only in the neurons, but also in the non-neuronal cells, such as pia mater, choroidal plexus, and pineal gland express galectin-1 mRNAs, although the physiological significance has not been elucidated.

Previously, galectin-1 null mutant mice were generated by homologous recombination in ES cells. Following transfer of this mutation into the germ line, the mice bearing null galecti-1 were analyzed (Poirier and Robertson, 1993). Surprisingly, the mice lacking the galectin-1 protein appear to develop normally. Adult mutant mice do not harbor any obvious phenotypic differences that distinguish them from wild-type siblings, although the further investigation using these null mutants will be required to reveal the physiological function of galectin-1 in the nervous system.

Recently, another protein family was found to share similar properties with galectin family in some respects, although they are not structurally related. Annexins, which had been previously considered as phospholipid-binding proteins, display a glycosaminoglycan-binding activity, and thus turned out to be new lectin molecules. Annexin II has been described as a regulatory factor that facilitates the expression of sensory neuron-specific tetrodotoxin-resistant sodium channel (Okuse et al., 2002). Annexin II light chain directly binds to the amino terminus of NaC1.8 and promotes the translocation of NaV1.8 to the plasma membrane to form a functional channel in response to tissue damage combined with growth factors such as NGF and TGF-α. Taken together the axonal growth activity of gaclectin-1, animal lectins may constitute a reactive pathway in the nervous system and play an important role in the nerve regeneration.

The expression of galectin-1 mRNA in the neurons of facial nuclei was transiently upregulated 6–9 h after facial nerve axotomy. This result suggests that the facial nerve injury can trigger the synthesis of galectin-1 in the neuronal cell bodies. The physiological role of this upregulation was not elucidated. In some cases, the upregulated galectin-1 may play a role in the inflammatory response after injury. The anti-inflammatory effect of galectin-1 was previously reported including the inhibition of chemical mediators of the inflammatory response (Rabinovich et al., 2000). It is also possible that upregulation of galectin-1, similar to neurotrophic factors and cytokines (Carlson et al., 1996; Lee et al., 1998), may help neuronal cells survive and regenerate neurites (Nishioka et al., 2002). Furthermore, upregulation of galectin-1 mRNA may increase galectin-1 in facial nerves resulting with increase of galectin-1 secretion. Some of secreted galectin-1 is briefly oxidized to become oxidized galectin-1 that loses lectin activity. Recent reports indicated that oxidized galectin-1 is essential *in vivo* for peripheral nerve regeneration after injury (Horie et al., 1999; Inagaki et al., 2000; Fukaya et al., 2002). Thus, oxidized galectin-1 could similarly work in facial motor neurons following facial nerve axotomy, although the precise mechanism how galectin-1 is secreted from neurons and other cells after axonal injury remains to be elucidated.

Acknowledgements—We thank Dr. Yoh Sasaki for technical assistance. We are indebted to Dr. Hitoshi Kawano, Tokyo Metropolitan Institute for Neuroscience, and Dr. Noboru Mizuno, National Institute for Physiological Science, for discussion and helpful comments. Grant Sponsor: Ministry of Health, Labor, and Welfare, Japan, Ministry of Education, Culture, Sports, Science and Technology, Japan, and the Sankyo Foundation of Life Science.

REFERENCES

Akazawa C, Shigemoto R, Bessho Y, Nakanishi S, Mizuno N (1994) Differential expression of five *N*-methyl-D-aspartate receptor subunit mRNAs in the cerebellum of developing and adult rats. J Comp Neurol 347:150–160.

Amano M, Calvan M, He J, Baum LG (2003) The ST6Gal I sialyltransferase selectively modifies *N*-glycans on CD45 to negatively regulate galectin-1-induced CD45 clustering, phosphatase modulation, and T cell death. J Biol Chem 278:7469–7475.

Barondes SH (1984) Soluble lectins: a new class of extracellular proteins. Science 223:1259–1264.

Barondes SH, Castronovo V, Cooper DW, Cummings RD, Drickamer K, Feizi T, Gitt MA, Hirabayashi J, Hughes C, Kasai K, Leffler H, Liu FT, Lotan R, Mercurio AM, Monsigny M, Pillai S, Poirier F, Raz A, Rigby PW, Rini JM, Wang JL (1994) Galectins: a family of animal β-galactoside-binding lectins. Cell 76:597–598.

Carlson CD, Bai Y, Ding M, Jonakait GM, Hart RP (1996) Interleukin-1 involvement in the induction of leukemia inhibitory factor mRNA

expression following axotomy of sympathetic ganglia. J Neuroimmunol 70:181–190.

Caron M, Bladier D, Joubert R (1990) Soluble galactoside-binding vertebrate lectins: a protein family with common properties. Int J Biochem 22:1379–1385.

Cooper DNW, Barondes SH (1990) Evidence for export of a muscle lectin from cytosol to extracellular matrix and for novel secretory mechanism. J Cell Biol 110:1681–1691.

Drickamer K (1988) Two distinct classes of carbohydrate-recognition domain in animal lectins. J Biol Chem 263:9557–9560.

Fukaya K, Hasegawa M, Mashitani T, Kadoya T, Horie H, Hayashi Y, Fujisawa H, Tachibana O, Kida S, Yamashita J (2003) Oxidized galectin-1 stimulates the migration of Schwann cells from both proximal and distal stumps of transected nerves and promotes axonal regeneration after peripheral nerve injury. J Neuropathol Exp Neurol 62:162–172.

Hirabayashi J, Kasai K (1993) The family of metazoan metal-independent β-galactoside-binding lectins; structure, function and molecular evolution. Glycobiology 3:297–304.

Horie H, Inagaki Y, Sohma Y, Nozawa R, Okawa K, Hasegawa M, Muramatsu N, Kawano H, Horie M, Koyama H, Sakai I, Takeshita K, Kowada Y, Takano M, Kadoya T (1999) Galectin-1 regulates initial axonal growth in peripheral nerves after axotomy. J Neurosci 19:9964–9974.

Hynes MA, Gitt M, Barondes SH, Jessell TM, Buck LB (1990) Selective expression of an endogenous lactose-binding lectin gene in subsets of central and peripheral neurons. J Neurosci 10:1004–1013.

Inagaki Y, Sohma Y, Horie H, Nozawa R, Kadoya T (2000) Oxidized galectin-1 promotes axonal regeneration in peripheral nerves but does not possess lectin properties. Eur J Biochem 267:2955–2964.

Lasky LA (1992) Selectins: interpreters of cell-specific carbohydrate information during inflammation. Science 258:964–969.

Lee SE, Shen H, Taglialatela G, Chung JM, Chung K (1998) Expression of nerve growth factor in the dorsal root ganglion after peripheral nerve injury. Brain Res 796:99–106.

Nishioka T, Sakumi K, Miura T, Tahara K, Horie H, Kadoya T, Nakabeppu Y (2002) FosB gene products trigger cell proliferation and morphological alteration with an increased expression of a novel processed form of galectin-1 in the rat 3Y1 embryo cell line. J Biochem (Tokyo) 131:653–661.

Okuse K, Malik-Hall M, Baker MD, Poon WYL, Kong H, Chao MV, Wood JN (2002) Annexin II light chain regulates sensory neuron-specific sodium channel expression. Nature 417:653–656.

Paxinos G, Watson C (1986) The rat brain in stereotaxic coordinates, 2nd edition. Sydney: Academic Press.

Poirier F, Robertson EJ (1993) Normal development of mice carrying a null mutation in the gene encoding the L14 S-type lectin. Development 119:1229–1236.

Puche AC, Key B (1995) Identification of cells expressing galectin-1, a galactose-binding receptor, in the rat olfactory system. J Comp Neurol 357:513–523.

Rabinovich GA, Sotomayor CE, Riera CM, Bianco I, Correa SG (2000) Evidence of a role for galectin-1 in acute inflammation. Eur J Immunol 30:1331–1339.

(Accepted 28 January 2004)

American Journal of Pathology, Vol. 164, No. 1, January 2004

Role of Ubiquitin Carboxy Terminal Hydrolase-L1 in Neural Cell Apoptosis Induced by Ischemic Retinal Injury *in Vivo*

Takayuki Harada,*† Chikako Harada,*† Yu-Lai Wang,* Hitoshi Osaka,*‡ Kazuhito Amanai,† Kohichi Tanaka,†‡ Shuichi Takizawa,* Rieko Setsuie,*§ Mikako Sakurai,*§ Yae Sato,*§ Mami Noda,§ and Keiji Wada*

From the Department of Degenerative Neurological Diseases, National Institute of Neuroscience, National Center of Neurology and Psychiatry, Kodaira, Tokyo; Laboratory of Molecular Neuroscience,† School of Biomedical Science and Medical Research Institute, Tokyo Medical and Dental University, Tokyo; Precursory Research for Embryonic Science and Technology (PRESTO),‡ Japan Science and Technology Corporation (JST), Kawaguchi, Saitama; Laboratory of Pathophysiology,§ Graduate School of Pharmaceutical Sciences, Kyushu University, Higashi-ku, Fukuoka, Japan*

Ubiquitin is thought to be a stress protein that plays an important role in protecting cells under stress conditions; however, its precise role is unclear. Ubiquitin expression level is controlled by the balance of ubiquitinating and deubiquitinating enzymes. To investigate the function of deubiquitinating enzymes on ischemia-induced neural cell apoptosis *in vivo*, we analyzed gracile axonal dystrophy (*gad*) mice with an exon deletion for ubiquitin carboxy terminal hydrolase-L1 (UCH-L1), a neuron-specific deubiquitinating enzyme. In wild-type mouse retina, light stimuli and ischemic retinal injury induced strong ubiquitin expression in the inner retina, and its expression pattern was similar to that of UCH-L1. On the other hand, *gad* mice showed reduced ubiquitin induction after light stimuli and ischemia, whereas expression levels of antiapoptotic (Bcl-2 and XIAP) and prosurvival (brain-derived neurotrophic factor) proteins that are normally degraded by an ubiquitin-proteasome pathway were significantly higher. Consistently, ischemia-induced caspase activity and neural cell apoptosis were suppressed ~70% in *gad* mice. These results demonstrate that UCH-L1 is involved in ubiquitin expression after stress stimuli, but excessive ubiquitin induction following ischemic injury may rather lead to neural cell apoptosis *in vivo*. (Am J Pathol 2004, 164:59–64)

The small 76 amino acid protein ubiquitin plays a critical role in many cellular processes, including cell cycle control, transcriptional regulation, and synaptic development.[1,2] Although ubiquitin has been identified as a heat shock- and stress-regulated protein in several kinds of cells,[3,4] recent studies have shown that ubiquitin promotes either cell survival or apoptosis, depending on the stage of cell development or other cellular factors.[5–8] Ubiquitin expression level is controlled by the balance of ubiquitinating enzymes: ubiquitin-activating (E1), ubiquitin-conjugating (E2), ubiquitin-ligase (E3) enzymes, and deubiquitinating enzymes (DUBs). DUBs are subdivided into ubiquitin carboxy terminal hydrolases (UCHs) and ubiquitin-specific proteases (UBPs). Mammalian UCHs, UCH-L1, and UCH-L3 are both small proteins of ~220 amino acids that share >40% amino acid sequence identity.[9] However, the distribution of these isozymes is quite distinct in that UCH-L3 is distributed ubiquitously while UCH-L1 is selectively expressed in neuronal cells and in the testis/ovary.[9,10] UCH-L1 constitutes ~5% of the brain's total soluble protein, which demonstrates a possibility that it plays a major role in neuronal cell function.[11] Indeed, UCH-L1 is a constituent of cellular aggregates that are indicative of neurodegenerative disease, such as Lewy bodies in Parkinson's disease.[12] Furthermore, an isoleucine to methionine substitution at amino acid 93 of UCH-L1 is reported in a family with a dominant form of Parkinson's disease.[13] Recently, we found a UCH-L1 gene exon deletion in mice that causes gracile axonal dystrophy (*gad*), a recessive neurodegenerative disease.[14] These examples of neurodysfunction from UCH-L1 mutations in both humans and mice prompted us to investigate the function of UCH-L1 in ischemia-induced neuronal cell apoptosis. For this purpose, we evaluated the extent of ischemic injury in wild-type and *gad* mice retina. The retina was chosen as a model be-

Supported by grants from the Organization for Pharmaceutical Safety and Research, Japan Science and Technology Cooperation, the Ministry of Health, Labor and Welfare of Japan, and the Ministry of Education, Culture, Sports, Science and Technology of Japan.

C. H. was supported by the Japan Society for the Promotion of Science for Young Scientists.

Accepted for publication September 10, 2003.

Address reprint requests to Keiji Wada, M.D., Ph.D., Department of Degenerative Neurological Diseases, National Institute of Neuroscience, NCNP, 4-1-1 Ogawahigashi, Kodaira, Tokyo 187-8502, Japan. E-mail: wada@ncnp.go.jp.

cause it is a highly organized neural tissue. In addition, its layered construction is suitable for analysis of cell type-specific biological response against diverse stimuli.[15–18] Here, we show that the absence of UCH-L1 partially prevents ischemia-induced retinal cell apoptosis and propose its possible mechanisms.

Materials and Methods

Animals

We used homozygous *gad* mice[14] and their wild-type littermates between postnatal days 35 and 56. The *gad* mouse was found in the F2 offspring of CBA and RFM inbred strain mice and has been maintained by brother-sister mating for more than 10 years.[19] Mice were maintained and propagated at the National Institute of Neuroscience, National Center of Neurology and Psychiatry (Japan). Experiments using the mice were approved by the Animal Investigation Committee of the Institute. The animals were housed in a room with controlled temperature and fixed lighting schedule. Light intensity inside the cages ranged from 100 to 200 lux. For the analysis of light stress, the pupils were dilated with 0.5% phenylephrinezhydrochloride and 0.5% tropicamide, and the mice were exposed to 800~1300 lux of white fluorescent light for 30 minutes. Animals for negative controls were dark-adapted for 12 hours, and sacrificed under dim red light.

Immunohistochemistry

Animals were anesthetized with diethylether and perfused transcardially with saline, followed by 4% paraformaldehyde in 0.1 mol/L phosphate buffer containing 0.5% picric acid at room temperature. The eyes were removed and postfixed overnight in the same fixative at 4°C and embedded in paraffin wax. The posterior part of the eyes were sectioned saggitally at 7-μm thickness through the optic nerve, mounted and stained with hematoxylin and eosin. For immunohistochemical staining, the sections were incubated with phosphate-buffered saline (PBS) containing 10% normal donkey serum for 30 minutes at room temperature. They were then incubated overnight with a rabbit polyclonal antibody against ubiquitin (1:600; Chemicon, Temecula, CA) or mouse monoclonal antibody against UCH-L1 (1:200; Medac, Wedel, Germany). They were then visualized with fluorescein isothiocyanate (FITC)-conjugated goat anti-rabbit or anti-mouse IgG (Jackson Immunoresearch, West Grove, PA), respectively. The sections were examined by a confocal laser scanning microscope (Olympus, Tokyo, Japan).

Histology and Morphometric Studies

Ischemia was achieved and the animals were sacrificed as previously described.[16,17] Briefly, we instilled sterile saline into the anterior chamber of the left eye at 150 cm H_2O pressure for 15 minutes while the right eye served as a non-ischemic control. The animals were sacrificed 1 or 7 days after reperfusion, and eyes were enucleated for histological and morphometric studies. The posterior part of the eyes was sectioned sagittally at 7-μm thickness through the optic nerve, mounted and stained with hematoxylin and eosin. Ischemic damage after 7 days was quantified in two ways. First, the thickness of the inner retinal layer (IRL) [from the ganglion cell layer (GCL) to the inner nuclear layer (INL)] was measured with a calibrated reticle at ×80. Second, in the same sections, the number of cells in the GCL was counted from one ora serrata through the optic nerve to the other ora serrata. The changes of the number of ganglion cells after ischemia were expressed in ratio compared with the non-ischemic fellow eyes.

TUNEL Staining

Sections were incubated in 0.26 U/μl TdT in the supplied 1X buffer (Invitrogen, Carlsbad, CA), and 20 μmol/L biotinylated-16-dUTP (Roche, Basel, Switzerland) for 60 minutes at 37°C. Sections were washed three times in PBS (pH 7.4) and blocked for 30 minutes with 2% bovine serum albumin in PBS (pH 7.4). The sections were then incubated with FITC-coupled streptavidin (Jackson Immunoresearch), diluted 1:100 in PBS for 30 minutes, and examined with a confocal laser scanning microscope (Olympus).

Quantification of Retinal Cell Apoptosis and Caspase Activities

A mouse retina 1 day after ischemia was homogenized in 100 μl PBS containing 1 mmol/L phenylmethyl sulfonyl fluoride and centrifuged at 15,000 × *g* for 10 minutes. A portion of supernatant was used to quantify protein concentration, and the rest was processed for assays. Retinal cell apoptosis was quantified using the Cell Death ELISA kit (Roche). Caspase-1- and caspase-3-like activities were measured using caspase-1 and caspase-3 Colorimetric Assay Kits (Bio-vision, Mountain View, CA), respectively.

Western Blot Analysis

Western blots were performed as previously reported.[14] Five micrograms of total protein were loaded per lane. Primary antibodies used were Bcl-2 (1:500), Bcl-xL (1:500), XIAP (1:500) (all from Transduction Laboratories, Franklin Lakes, NJ), phosphorylated cyclic AMP responsive element-binding protein (PCREB) (1:500; Upstate Biotechnology, Waltham, MA) and brain-derived neurotrophic factor (BDNF) (1:500; Santa Cruz Biotechnology, Santa Cruz, CA). Blots were further incubated with an anti-mouse or rabbit IgG-horseradish peroxidase conjugate (1:10000; Chemicon). The Super Signal detection kit (Pierce, Rockford, IL) was used for visualization of immunoreactive bands.

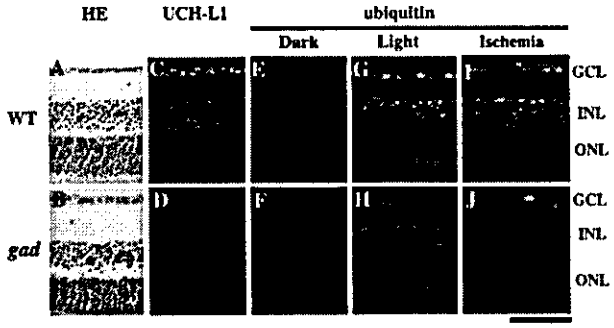

Figure 1. Functional loss of UCH-L1 decreases light- and ischemia-induced ubiquitin induction *in vivo*. Hematoxylin and eosin (HE) staining (**A** and **B**), immunostaining of UCH-L1 (**C** and **D**), immunostaining of ubiquitin in dark-reared (**E** and **F**), light-stressed (**G** and **H**) and ischemic (**I** and **J**) retina in wild-type (**A**, **C**, **E**, **G**, and **I**) and *gad* (**B**, **D**, **F**, **H**, and **J**) mice. Retinal structure is normal (**B**), but stress-induced ubiquitin induction is reduced (**H** and **J**) in *gad* mice. For the analysis of light stress (**G** and **H**), mice were exposed to 800 to 1300 lux of light for 30 minutes. Animals for negative controls were dark-adapted for 12 hours, and sacrificed under dim red light (**E** and **F**). Ischemic retina was prepared 1 day after ischemic injury (**I** and **J**). Bar, 50 μm.

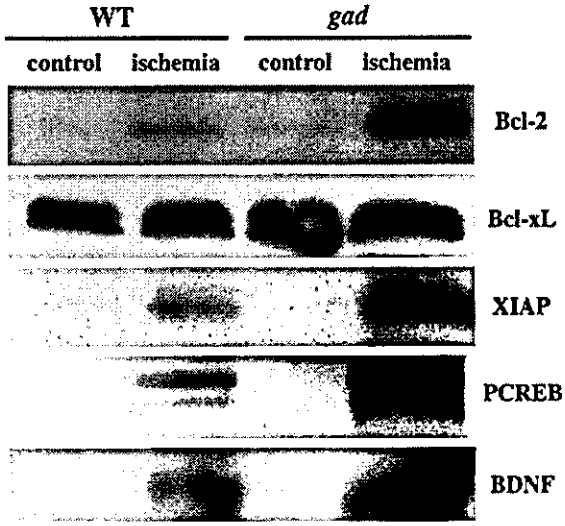

Figure 2. Immunoblot analysis of antiapoptotic and prosurvival proteins after ischemic injury. Five micrograms of total protein were prepared from whole retinas before (control) and 1 day after ischemic injury (ischemia). Representative image of four independent experiments are shown.

Results

Effect of UCH-L1 on Retinal Structure and Ubiquitin Expression

To determine the effect of UCH-L1 on retinal morphology, we examined the retinal tissue of *gad* mice with a UCH-L1 gene exon deletion.[14] Retinal structure in *gad* mice (Figure 1B) was normal compared with wild-type mice (Figure 1A). UCH-L1-like immunoreactivity was observed in the ganglion cell layer (GCL) and the inner nuclear layer (INL) in wild-type mice (Figure 1C) but was absent in *gad* mice (Figure 1D). Since ubiquitin is thought to be a stress protein,[1,20] we first examined the effect of the common oxidative stress for eye tissues, light stimuli, on ubiquitin induction.[20] Interestingly, ubiquitin was almost absent in both groups of animals, following dark adaptation (Figure 1, E and F). However, light stimuli strongly induced ubiquitin expression in the GCL and INL in wild-type mice (Figure 1G) but its induction level was very low in *gad* mice (Figure 1H). Ubiquitin expression pattern in wild-type mice was similar to that of UCH-L1 (Figure 1C). We next examined the effect of ischemia, severe oxidative stress,[21,22] on ubiquitin induction. As with light stimuli, ischemia induced strong ubiquitin expression in the GCL and INL (Figure 1I) and its induction was suppressed in *gad* mice (Figure 1J). These results demonstrate that retinal UCH-L1 plays an important role in ubiquitin induction[11] and *gad* mice retina is a useful model to investigate the effects of UCH-L1 on ischemic injury *in vivo*.

Effect of UCH-L1 on Antiapoptotic and Prosurvival Protein Expressions Following Ischemic Injury

The ubiquitin-proteasome pathway might be involved in non-neural cell apoptosis because this pathway can degradate antiapoptotic proteins such as Bcl-2 and XIAP *in vitro*.[5–8] To determine whether this is true for retinal cell apoptosis *in vivo*, we examined their protein expression levels in ischemic retinas (Figure 2). Ischemia-induced Bcl-2 protein level in *gad* mice was substantially higher than that of wild-type mice. Bcl-xL proteins (antiapoptotic member in the Bcl-2 family)[23,24] were examined at the same time as a control, but no obvious alternations were noted. On the other hand, XIAP protein[25,26] expression was apparently higher in *gad* mice. In addition to oxidative stress, ischemia induces calcium influx in neurons and triggers phosphorylation of cyclic AMP responsive element-binding protein (CREB).[27] PCREB can activate transcription of trophic factor proteins, such as BDNF, by binding to a critical calcium response element.[27] Since CREB is degraded by a ubiquitin-proteasome pathway by a phosphorylation-dependent mechanism,[28] we hypothesized a similar degradative pathway for CREB in ischemic retina. In wild-type mice, ischemia increased PCREB, but its expression level was much higher in *gad* mice. Consistent with PCREB up-regulation, BDNF protein expression was also higher in *gad* mice. Thus, excessive ubiquitin induction after ischemic injury may lead to the degradation of antiapoptotic proteins and suppression of the transcription of prosurvival proteins.[5–8,28]

Effect of UCH-L1 on Ischemia-Induced Neural Cell Apoptosis

To determine whether increased expression of antiapoptotic and prosurvival proteins in *gad* mice really leads to resistance against ischemia, we next examined the histology of ischemic retinas in both strains. As expected, ischemic damage in *gad* mice was mild compared with wild-type mice (Figure 3); the thickness of the inner retinal layer (IRL) (Figure 4A) and the percentage of surviving cells in the GCL (Figure 4B) after ischemia were significantly larger in *gad* mice. We also analyzed apoptotic cells in the retina by TUNEL staining. Control animals

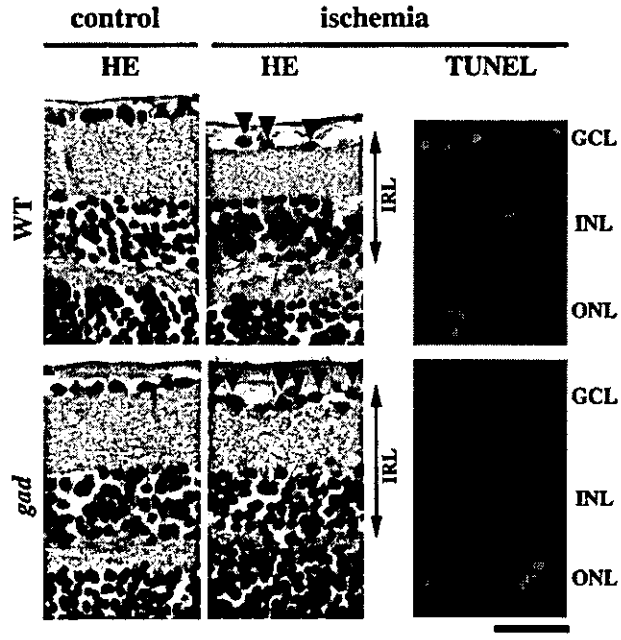

Figure 3. Representative pictures of HE staining (**left**) and TUNEL staining (**right**) in wild-type and *gad* mice retina before (control) and after ischemic injury (ischemia). Retinal damage 7 days after ischemia (HE staining) in *gad* mice was mild compared with wild-type mice. Consistently, TUNEL-positive cells 1 day after ischemia were observed only in the ONL in *gad* mice. Bar, 50 μm.

showed practically no signals in both strains (data not shown). However, in ischemic retinas, TUNEL-positive cells were observed in all three nuclear layers in wild-type mice, but mainly only in the outer nuclear layer (ONL) in *gad* mice (Figure 3). Consistently, quantitative analysis by ELISA demonstrated decreased retinal cell apoptosis in *gad* mice (Figure 4C). Ischemia-induced retinal cell apoptosis is executed by two distinct caspase proteases.

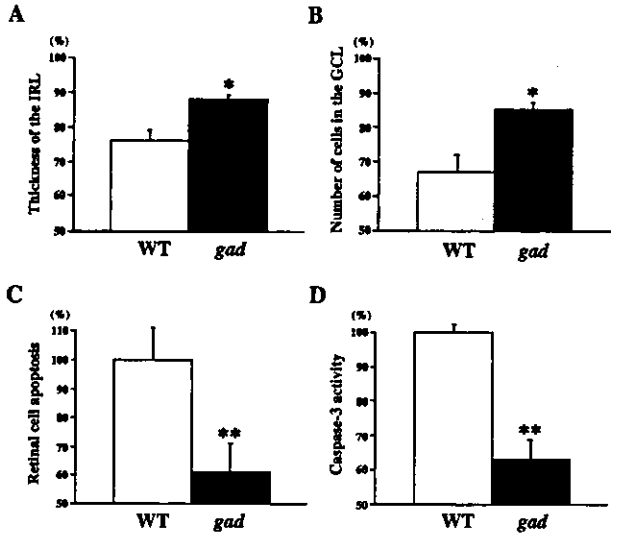

Figure 4. Effect of ischemic injury in wild-type and *gad* mice retina. Thickness of the IRL (arrows in Figure 3) (**A**) and the number of cells in the GCL (arrowheads in Figure 3) (**B**) in retina 7 days after ischemic injury as a percentage of the non-ischemic fellow eye. Quantitative analysis of retinal cell apoptosis (**C**) and caspase-3-like activity (**D**) in retina 1 day after ischemic injury. Results of six independent experiments are presented as mean ± SD (*, $P < 0.05$; **, $P < 0.01$).

Caspase-1 is predominantly associated with photoreceptor cell apoptosis in the ONL, whereas caspase-3 is more active in the GCL and INL for the same process.[29] To determine the mechanisms of strong tolerance against ischemia in *gad* mice, we next examined the activity of these two caspases in the ischemic retina. Caspase-1-like activity was not significantly different in *gad* mice compared with wild-type mice (80 ± 13%; P = not significant) (data not shown). On the other hand, caspase-3-like activity in *gad* mice was suppressed to 63 ± 6% compared with wild-type mice ($P < 0.01$) (Figure 4D).

Discussion

Ischemic injury is mainly associated with excessive concentrations of glutamate, which results in overactivation of glutamate receptors and initiates a cascade of events that leads to necrosis and/or apoptosis. Consistently, several studies have shown that retinal neurons can be protected by glutamate receptor antagonists.[17,30,31] An alternative strategy to attenuate glutamate neurotoxicity is keeping the extracellular glutamate concentration below neurotoxic levels. We previously demonstrated that selective inhibition of N-acetylated-α-linked-acidic dipeptidase (NAALADase), an enzyme responsible for the hydrolysis of neuropeptide N-acetyl-aspartyl-glutamate to N-acetyl-aspartate and glutamate, robustly protects neurons in a rat model of stroke[32] and in a mouse model of ischemic retinal injury.[17] Another possible target is the glutamate transporter.[33] There are four subtypes of glutamate transporters (GLAST, GLT-1, EAAC1, and EAAT5) in the retina.[16,33] By using GLAST and GLT-1 knockout mice,[34,35] we showed that both GLAST and GLT-1 (GLAST > GLT-1) are crucial for the protection of retinal cells from ischemic injury.[16]

In addition to these typical molecules involved in glutamate neurotoxicity, we first demonstrated that neuron-specific deubiquitinating enzyme, UCH-L1, is a new possible therapeutic target for ischemic retinal injury. In *gad* mice, functional loss of UCH-L1 results in the protection of retinal neurons following ischemic injury. One of the possible mechanisms is the accumulation of antiapoptotic proteins Bcl-2 and XIAP. Suppression of Bcl-2 leads to altered mitochondrial membrane permeability resulting in release of cytochrome c into the cytosol, which can trigger caspase activation leading to apoptosis.[23–26] On the other hand, a member of the IAP (inhibitor of apoptosis proteins) family, XIAP, can bind to and inhibit caspase-3 activation.[23–26] Consistently, retinal cell apoptosis in *gad* mice is suppressed mainly in the inner retina (Figure 3), where caspase-3 is more active than caspase-1.[27] These results suggest a possibility that functional loss of UCH-L1 may lead to decreased cytochrome c release from mitochondria and subsequent caspase inactivation in *gad* mice. If UCH-L1 inhibition works on the apoptotic pathway both before and after cytochrome c release from mitochondria,[23–26] this method may have a broader effect compared with the overexpression or suppression of a single antiapoptotic or apoptotic factor, respectively.

On the other hand, BDNF and PCREB protein expression levels were also up-regulated in *gad* mice. Recent studies have shown that trophic factors such as BDNF, ciliary neurotrophic factor (CNTF), basic fibroblast growth factor (bFGF), or glial cell line-derived neurotrophic factor (GDNF) increase RGC survival and regeneration.[36–45] Since CREB plays a central role in mediating responses of trophic factors including BDNF,[27] enhanced release of these trophic factors in *gad* mice may prevent ischemia-induced retinal cell apoptosis. We previously showed that, in addition to direct neuroprotection, these factors can alter secondary trophic factor production in retina-specific Müller glial cells, which indirectly regulate neural cell survival.[18,46] Consistently, intraocular injection of trophic factors induces the phosphorylated form of extracellular receptor kinase (pERK) or c-fos mainly in Müller cells.[47,48] Thus, loss of UCH-L1 may induce neural cell survival by stimulating both neural and glial cells.[18,46,49]

Ischemic retinal injury is implicated in a number of pathological states, such as retinal artery occlusion, glaucoma, and diabetic retinopathy.[16,17,30,31] Accordingly, the present results raise intriguing possibilities for the management of these pathological conditions by modifying the expression of UCH-L1 and activity of the ubiquitin-proteasome pathway.[50] Using this strategy with trophic factors,[18,46] NAALADase inhibitor,[17] glutamate transporter activators, such as bromocryptine,[51,52] or overexpression of GLAST or GLT-1,[16] may induce synergic effects on multiple cellular targets to prevent ischemia-induced neural cell apoptosis. However, due to the central function of the ubiquitin system in many basic cellular processes, modulation of this system can become a "double-edged sword".[1] Depletion of the free ubiquitin pool may cause accumulation of proteins that should be subjected to ubiquitin-dependent proteolysis. To address these critical issues, further investigations revealing the functional site of UCH-L1 and its involvement in ubiquitin induction *in vivo* will be needed.

Acknowledgments

We thank H.-M. A. Quah and L.F. Parada for critical reading of the manuscript, and members of the Wada lab for helpful discussions.

References

1. Hershko A, Ciechanover A, Varshavsky A: The ubiquitin system. Nat Med 2000, 6:1073–1081
2. DiAntonio A, Haghighi AP, Portman SL, Lee JD, Amaranto AM, Goodman CS: Ubiquitination-dependent mechanisms regulate synaptic growth and function. Nature 2001, 412:449–452
3. Finley D, Ozkaynak E, Varshavsky A: The yeast polyubiquitin gene is essential for resistance to high temperatures, starvation, and other stresses. Cell 1987, 48:1035–1046
4. Bond U, Agell N, Haas AL, Redman K, Schlesinger MJ: Ubiquitin in stressed chicken embryo fibroblasts. J Biol Chem 1988, 263:2384–2388
5. Dimmeler S, Breitschopf K, Haendeler J, Zeiher AM: Dephosphorylation targets Bcl-2 for ubiquitin-dependent degradation: a link between the apoptosome and the proteasome pathway. J Exp Med 1999, 189:1815–1822
6. Breitschopf K, Haendeler J, Malchow P, Zeiher AM, Dimmeler S: Posttranslational modification of Bcl-2 facilitates its proteasome-dependent degradation: molecular characterization of the involved signaling pathway. Mol Cell Biol 2000, 20:1886–1896
7. Daino H, Matsumura I, Takada K, Odajima J, Tanaka H, Ueda S, Shibayama H, Ikeda H, Hibi M, Machii T, Hirano T, Kanakura Y: Induction of apoptosis by extracellular ubiquitin in human hematopoietic cells: possible involvement of STAT3 degradation by proteasome pathway in interleukin 6-dependent hematopoietic cells. Blood 2000, 95:2577–2585
8. Yang Y, Fang S, Jensen JP, Weissman AM, Ashwell JD: Ubiquitin protein ligase activity of IAPs and their degradation in proteasomes in response to apoptotic stimuli. Science 2000, 288:874–877
9. Wilkinson KD, Lee KM, Deshpande S, Duerksen-Hughes P, Boss JM, Pohl J: The neuron-specific protein PGP 9.5 is a ubiquitin carboxyl-terminal hydrolase. Science 1989, 246:670–673
10. Wilkinson KD, Deshpande S, Larsen CN: Comparisons of neuronal (PGP 9.5) and non-neuronal ubiquitin C-terminal hydrolases. Biochem Soc Trans 1992, 20:631–637
11. Osaka H, Wang YL, Takada K, Takizawa S, Setsuie R, Li H, Sato Y, Nishikawa K, Sun YJ, Sakurai M, Harada T, Hara Y, Kimura I, Chiba S, Namikawa K, Kiyama H, Noda M, Aoki S, Wada K: Ubiquitin carboxy-terminal hydrolase L1 binds to and stabilizes monoubiquitin in neuron. Hum Mol Genet 2003, 12:1945–1958
12. Lowe J, McDermott H, Landon M, Mayer RJ, Wilkinson KD: Ubiquitin carboxyl-terminal hydrolase (PGP 9.5) is selectively present in ubiquitinated inclusion bodies characteristic of human neurodegenerative diseases. J Pathol 1990, 161:153–160
13. Leroy E, Boyer R, Auburger G, Leube B, Ulm G, Mezey E, Harta G, Brownstein MJ, Jonnalagada S, Chernova T, Dehejia A, Lavedan C, Gasser T, Steinbach PJ, Wilkinson KD, Polymeropoulos MH: The ubiquitin pathway in Parkinson's disease. Nature 1998, 395:451–452
14. Saigoh K, Wang YL, Suh JG, Yamanishi T, Sakai Y, Kiyosawa H, Harada T, Ichihara N, Wakana S, Kikuchi T, Wada K: Intragenic deletion in the gene encoding ubiquitin carboxy-terminal hydrolase in gad mice. Nat Genet 1999, 23:47–51
15. Harada T, Imaki J, Hagiwara M, Ohki K, Takamura M, Ohashi T, Matsuda H, Yoshida K: Phosphorylation of CREB in rat retinal cells after focal retinal injury. Exp Eye Res 1995, 61:769–772
16. Harada T, Harada C, Watanabe M, Inoue Y, Sakagawa T, Nakayama N, Sasaki S, Okuyama S, Watase K, Wada K, Tanaka K: Functions of the two glutamate transporters GLAST and GLT-1 in the retina. Proc Natl Acad Sci USA 1998, 95:4663–4666
17. Harada C, Harada T, Slusher BS, Yoshida K, Matsuda H, Wada K: N-acetylated-α-linked-acidic dipeptidase inhibitor has a neuroprotective effect on mouse retinal ganglion cells after pressure-induced ischemia. Neurosci Lett 2000, 292:134–136
18. Harada T, Harada C, Nakayama N, Okuyama S, Yoshida K, Kohsaka S, Matsuda H, Wada K: Modification of glial-neuronal cell interactions prevents photoreceptor apoptosis during light-induced retinal degeneration. Neuron 2000, 26:533–541
19. Yamazaki K, Wakasugi N, Tomita T, Kikuchi T, Mukoyama M, Ando K: Gracile axonal dystrophy (GAD), a new neurological mutant in the mouse. Proc Soc Exp Biol Med 1988, 187:209–215
20. Naash MI, Al-Ubaidi MR, Anderson RE: Light exposure induces ubiquitin conjugation and degradation activities in the rat retina. Invest Ophthalmol Vis Sci 1997, 38:2344–2354
21. Bonfoco E, Krainc D, Ankarcrona M, Nicotera P, Lipton SA: Apoptosis and necrosis: two distinct events induced, respectively, by mild and intense insults with N-methyl-D-aspartate or nitric oxide/superoxide in cortical cell cultures. Proc Natl Acad Sci USA 1995, 92:7162–7166
22. Szabo ME, Haines D, Garay E, Chiavaroli C, Farine JC, Hannaert P, Berta A, Garay RP: Antioxidant properties of calcium dobesilate in ischemic/reperfused diabetic rat retina. Eur J Pharmacol 2001, 428:277–286
23. Tsujimoto Y, Shimizu S: Bcl-2 family: life-or-death switch. FEBS Lett 2000, 466:6–10
24. Ranger AM, Malynn BA, Korsmeyer SJ: Mouse models of cell death. Nat Genet 2001, 28:113–118
25. Deveraux QL, Reed JC: IAP family proteins: suppressors of apoptosis. Genes Dev 1999, 13:239–252
26. Green DR: Apoptotic pathways: paper wraps stone blunts scissors. Cell 2000, 102:1–4